

HQSAR Study on Imidazo[1,2-b]pyridazine Derivatives as p38 MAP Kinase Antagonists

Swapnil P. Bhujbal¹, Seketoulie Keretsu¹, and Seung Joo Cho^{1,2*}

Abstract

p38 MAP kinase belongs to the Mitogen-activated protein (MAP) kinase family; a serine/threonine kinase. It plays an important role in intracellular signal transduction pathways. It is associated with the development and progression of various cancer types making it a crucial drug target. Present study involves the HQSAR analysis of recently reported imidazo[1,2-b]pyridazine derivatives as p38 MAP kinase antagonists. The model was generated with Atom (A), bond (B), chirality (Ch), and hydrogen (H) parameters and with different set of atom counts to improve the model. An acceptable HQSAR model ($q^2=0.522$, SDEP=0.479, NOC=5, $r^2=0.703$, SEE=0.378, BHL=97) was developed which exhibits good predictive ability. A contribution map for the most active compound (compound **17**) illustrated that hydrogen and nitrogen atoms in the ring A and ring B, as well as nitrogen atom in ring C and the hydrogen atom in the ring D provided positive activity in inhibitory effect while, the least active compound (compound **05**) possessed negative contribution to inhibitory effect. Hence, analysis of produced HQSAR model can provide insights in the designing potent and selective p38 MAP kinase antagonists.

Keywords: p38 MAP Kinase, HQSAR, Pyridazine Derivatives, p38 MAP Kinase Antagonists

1. Introduction

p38 MAP kinase is a member of the Mitogen-activated protein (MAP) kinase family. MAP kinases are serine/threonine kinases that mediate intracellular signal transduction pathways^[1,2]. It is widely expressed in endothelial, inflammatory and immune cells^[3]. The activation of p38 MAP kinases is normally associated with apoptosis. It is activated by inflammatory cytokines or extracellular stressors such as heat, mechanical wear, osmotic shock, and ultraviolet light. It is necessary for the lipopolysaccharide-induced translation of tumor necrosis factor in monocytes^[3,4]. It phosphorylates and activates transcription factors ATF-2, GADD153 and CHOP-1^[1,4,5]. p38 MAPK is composed of two domains, a 135-residue N-terminal domain, and a 225-residue C-terminal domain. The catalytic site is at the junction

between the two domains^[6]. The N-terminal domain is composed mainly of β -sheets, while the C-terminal domain is mostly helical. The N-terminal domain creates a binding pocket for the adenine ring of ATP, and the C-terminal domain contains the presumed catalytic base, phosphorylation lip, and magnesium binding sites^[1,6].

The p38 MAP kinase family consists of four isoforms^[7]. p38-MAPK α , p38-MAPK β , p38-MAPK γ , and p38-MAPK δ . Among all isoforms, p38 α is widely expressed and is the most abundant p38 isoform present in most cell types^[8]. p38 is phosphorylated and activated specifically by MEK3 and MEK6 and together with c-Jun N-terminal kinases 1 and 2 (JNK1 and JNK2) by MEK4^[9,10]. The mitogen-activated protein kinase pathway plays an important role in the development and progression of many cancer types such as prostate cancer, breast cancer, bladder cancer, liver cancer, lung cancer and leukemia^[8]. Therefore, it is considered that the p38 plays an important role in cancer and tumor formation.

Many inhibitors which are reported to target p38 MAP kinase have been in phase I and II clinical trials^[11]. Nevertheless, no inhibitors are FDA (The Food

¹Department of Biomedical Sciences, College of Medicine, Chosun University, Gwangju 501-759, Republic of Korea

²Department of Cellular Molecular Medicine, College of Medicine, Chosun University, Gwangju 501-759, Republic of Korea

*Corresponding author : chosj@chosun.ac.kr

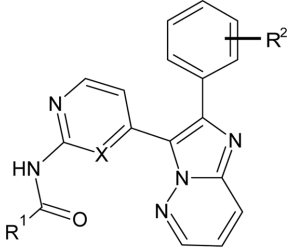
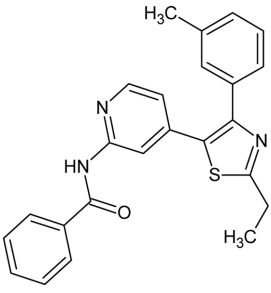
(Received : May 21, 2018, Revised : June 14, 2018,

Accepted : June 25, 2018)

and Drug Administration) approved or advanced to a final clinical stage. For example, two p38 inhibitors reported to be in clinical development are HEP689 and VX-745^[12]. Potent anti-inflammatory activity has been disclosed for HEP689, and the compound as entered clinical development for the treatment of psoriasis and

other skin disorders. VX-745 is in Phase II trials for rheumatoid arthritis. Furthermore, several p38 kinase inhibitors such as CNI-1493, SB 203580 and SB 220025 were confirmed in preclinical studies for their therapeutic potential in murine models of collagen-induced arthritis were successful^[12,13]. Most of these

Table 1. Structure and biological activity values of imidazo[1,2-b]pyridazine derivatives as p38 MAP kinase inhibitors

				
Compound	X	R ¹	R ²	pIC ₅₀ (nM)
1				6.620
2	CH	Ph	3-Me	7.137
3	N	Ph	3-Me	7.252
4	CH	Ph	3-Cl	7.469
5	CH	Ph	4-Cl	6.538
6	CH	Ph	3-Me, 4-F	8.027
7	CH	3-CF ₃ -Ph	3-Me, 4-F	7.959
8	CH	3-CF ₃ -Ph	3-Cl, 4-F	6.678
9	CH	2-CH ₃ -Ph	3-Me, 4-F	7.076
10	CH	3-CH ₃ -Ph	3-Me, 4-F	7.959
11	CH	4-CH ₃ -Ph	3-Me, 4-F	7.638
12	CH	3-F-Ph	3-Me, 4-F	7.921
13	CH	3-Cl-Ph	3-Me, 4-F	7.854
14	CH	2-Py	3-Me, 4-F	7.638
15	CH	3-Py	3-Me, 4-F	8.658
16	CH	4-Py	3-Me, 4-F	8.268
17	CH	6-Me-3-Py	3-Me, 4-F	8.745
18	CH	2-Me-4-Py	3-Me, 4-F	8.357
19	CH	6-Me-3-Py <i>N</i> -oxide	3-Me, 4-F	8.569
20	CH	2-Me-4-Py <i>N</i> -oxide	3-Me, 4-F	8.268

inhibitors failed due to either poor efficacy or toxicity.

Thus, it is crucial to design potent and selective p38 MAP kinase inhibitors. In the present work, HQSAR (Hologram Quantitative Structure-Activity Relationship) was used to generate a model to identify the vital group or atom that caused inhibition of p38. Our results could be useful to find novel and unique p38 MAP kinase inhibitors.

2. Methodology

2.1. Dataset

A series of imidazo[1,2-b]pyridazine derivatives reported as potent p38 MAP kinase inhibitors (20 compounds) were taken for the HQSAR study^[3] and were shown in Table 1. All the 20 compounds were sketched and optimized by energy minimization with tripos force field using SYBYL-X 2.1^[14]. Gasteiger-Hückel charges were applied as partial charges. The biological data expressed as IC₅₀ values (nM) were converted into pIC₅₀ (-log IC₅₀) values. The dataset was then used for HQSAR analysis.

2.2. HQSAR

HQSAR has the capacity to quickly and effectively produce QSAR models of high statistical quality and predictive value. HQSAR does not need a 3D structure of bioactive conformation or molecular alignments. HQSAR model generation deals with the 2D structure directed fragment fingerprint. These molecular finger-

prints are broken into strings at fixed intervals as specified by a hologram length (HL) parameter. The HL decides the number of bins in the hologram into which the fragments are hashed. The best possible HQSAR model was generated from screening through the 12 default HL values ranging from 53-401. The parameters such as atom (A), bond (B), connection (C), chirality (Ch), hydrogen (H) and donor/acceptor (DA) were used for the model development. The validity of the model depends on statistical parameters such as r^2 , q^2 by Leave-one-out (LOO)^[15].

3. Results and Discussion

3.1. HQSAR Analysis

The HQSAR model with acceptable predictive ability with regard to q^2 and r^2 was developed. Models were developed using parameters such as Atom (A), bond (B) connection (C), chirality (Ch), hydrogen (H) and donor/acceptor (DA) with different hologram lengths. Among all, the model with A/B/H/Ch combination possessed a q^2 of 0.522 and an r^2 of 0.703 with 0.479 as a standard error of prediction and 0.378 as a standard error of estimate. The statistical values of the model obtained were found to be reasonable and are depicted in Table 2. The actual and predicted activity values for the selected model are given in Table 4. The scatter plot for the same is shown in Fig. 1. The highest q^2 value obtained for parameters A/B/H/Ch was explored with an optional atom count (1-11) for further enhancement

Table 2. HQSAR models with different statistical parameters

Model	Fragment distinction	NOC	q^2	SDEP	r^2	SEE	BHL
1.	A/C/DA	2	0.397	0.539	0.560	0.460	257
2.	C/Ch/DA	2	0.320	0.572	0.456	0.512	199
3.	A/B/C/H	4	0.511	0.485	0.660	0.405	97
4.	A/B/H/Ch	5	0.522	0.479	0.703	0.378	97
5.	A/B/H/DA	5	0.517	0.482	0.657	0.407	353
6.	B/C/Ch/DA	2	0.303	0.579	0.472	0.504	353
7.	A/B/C/Ch/DA	2	0.361	0.555	0.538	0.472	353
8.	A/B/C/H/Ch	4	0.511	0.485	0.660	0.405	97
9.	A/B/C/H/DA	4	0.502	0.489	0.614	0.431	151
10.	A/B/C/H/DA/Ch	3	0.497	0.492	0.612	0.432	151

A=atom, B=bond, C=connection, H=hydrogen, Ch=chirality, DA=hydrogen bond donor/acceptor, NOC=number of components, q^2 =cross-validated correlation coefficient, SDEP=cross-validated standard error of prediction, r^2 =non-cross-validated correlation coefficient, SEE=standard error of estimate, BHL=best hologram length. Model selected to exploit atom count parameter is shown in **bold** face.

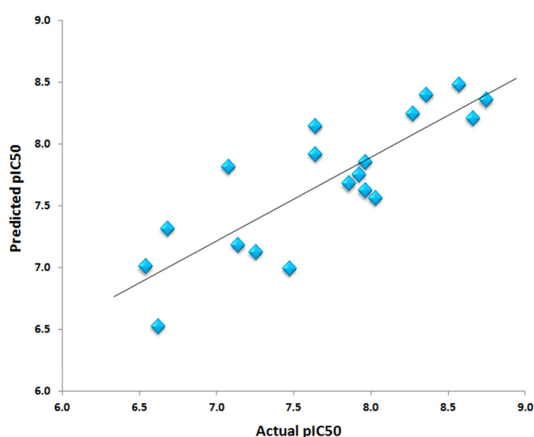


Fig. 1. Scatter plot diagram for HQSAR analysis. Plot shows the actual vs predicted pIC_{50} values of compounds.

of q^2 . The best statistical model was obtained with the default atom count (4-7) (Table 3). Atomic contributions in the HQSAR model were indicated using a standard color coding system (Fig. 2). A favorable or positive contribution to the activity was shown by yellow, green-blue and green color, while unfavorable and negative contribution to the activity was indicated by red, red-orange and orange colors. Molecules were selected based on their activity profile for the study of atomic contribution.

All the dataset compounds had a common substructure which varied in X, R¹, and R² substructure. Fig. 2a illustrates atom contribution map for the most active compound (compound 17). It shows that hydrogen atoms in the side chain and nitrogen atom of ring A, as well as nitrogen and hydrogen atoms of ring B showed positive contribution to the activity (pIC_{50} = 8.745).

Table 4. Actual pIC_{50} and predicted pIC_{50} with their residual values of selected HQSAR model.

Compound	Actual pIC_{50}	HQSAR	
		Predicted	Residual
1	6.620	6.521	0.099
2	7.137	7.181	-0.044
3	7.252	7.122	0.130
4	7.469	6.993	0.475
5	6.538	7.007	-0.469
6	8.027	7.560	0.467
7	7.959	7.620	0.339
8	6.678	7.313	-0.635
9	7.076	7.815	-0.739
10	7.959	7.853	0.106
11	7.638	7.914	-0.275
12	7.921	7.751	0.170
13	7.854	7.677	0.177
14	7.638	8.143	-0.504
15	8.658	8.204	0.453
16	8.268	8.244	0.024
17	8.745	8.355	0.390
18	8.357	8.396	-0.040
19	8.569	8.477	0.092
20	8.268	8.483	-0.215

Also, the nitrogen atoms of ring C and the hydrogen atom in the ring D contributed positively to the activity. While, the contribution map (Fig. 2b) for the least active compound (compound 05) signified that hydrogen atoms in the ring B and nitrogen atoms in the ring C contributed negatively to the activity (pIC_{50} = 6.538). No positive contribution from other atoms in the same rings was observed. Analysis of few compounds from active,

Table 3. Statistical summary of A/B/H/Ch model explored for the different atom counts.

Atom Count	NOC	q^2	SDEP	r^2	SEE	BHL
1-4	2	0.362	0.554	0.593	0.442	83
2-5	4	0.488	0.496	0.673	0.397	199
3-6	4	0.511	0.485	0.680	0.396	307
4-7	5	0.522	0.479	0.703	0.378	97
5-8	3	0.474	0.503	0.625	0.425	199
6-9	2	0.405	0.551	0.746	0.360	199
7-10	2	0.417	0.545	0.781	0.334	199
8-11	3	0.465	0.538	0.847	0.288	151

Final model selected for HQSAR analysis is represented in **bold**.

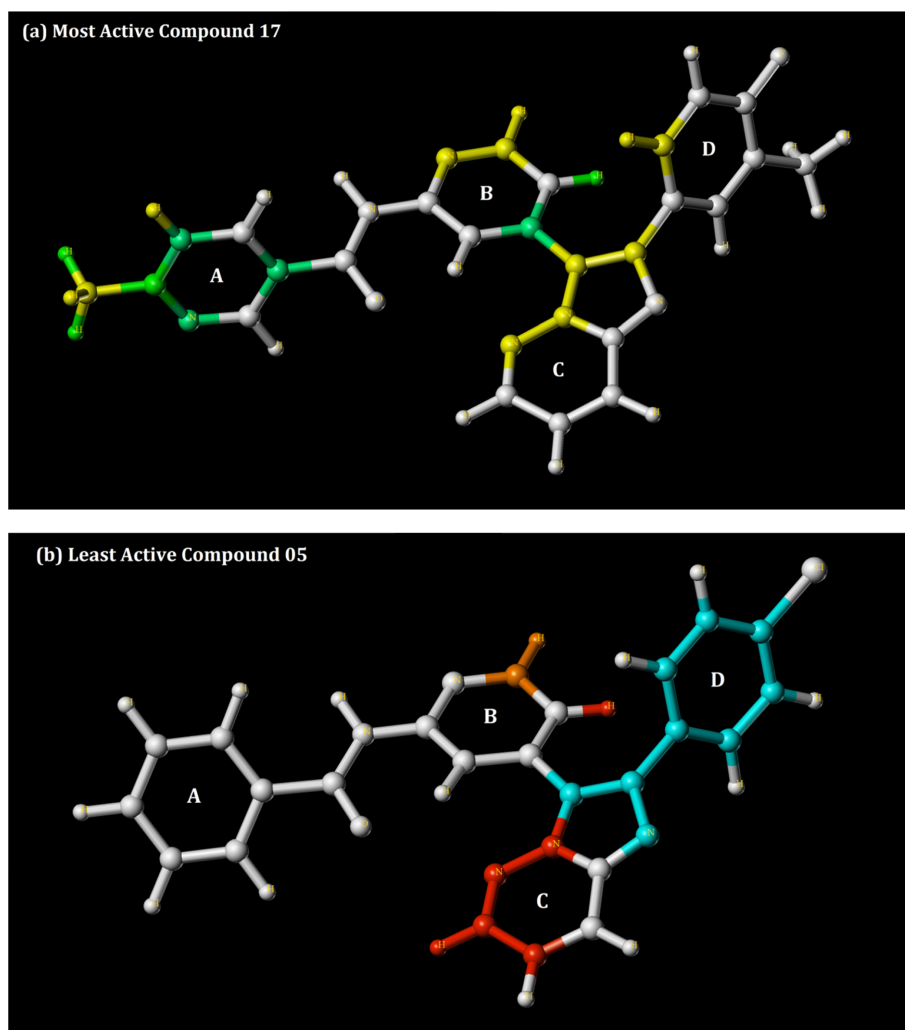


Fig. 2. HQSAR atomic contribution maps. (a) Map is shown for most active compound **17** and (b) least active compound **05**.

medium active and low active profile was also carried out to check their contribution in inhibitory effect. Compound **15** ($pIC_{50}=8.658$), which possess the second highest activity showed positive contribution from hydrogen atoms of ring A and nitrogen atom of ring B.

In contrast, medium active compound **13** ($pIC_{50}=7.854$) showed positive contribution from hydrogen atom of ring A and nitrogen atom of ring B with negative contribution from fluorine and hydrogen atoms of ring D. Whereas, compound from low active series such as compound **08** ($pIC_{50}=6.678$) showed negative contribution from hydrogen and nitrogen atoms of ring B

and C with no positive contribution from ring A and ring D. This might be the fact why these molecules reveal low activity and show less inhibitory effect as compared to medium and high active compounds.

4. Conclusion

The HQSAR analysis elucidates that the compound is highly active if the positive contribution from the atoms of particular ring (R group) is more. Medium active compounds have intermediate contribution as well as negative contribution in the activity. But, least

active compounds showed more negative contribution and had no positive contribution to the inhibitory effect. Fragment analyses of HQSAR can be performed as additional work to gain the compound modification guidelines. This could be supportive for designing novel high active compounds of the same series. Our HQSAR model helps to identify the functional groups & atoms and highlights their contribution to inhibitory potency.

Acknowledgements

This work is supported by the National Research Foundation of Korea (NRF), funded by the Ministry of Science and ICT (NRF-2015R1A5A2009070).

References

- [1] K. P. Wilson, M. J. Fitzgibbon, P. R. Caron, J. P. Griffith, W. Chen, P. G. McCaffrey, S. P. Chambers, and M. S.-S. Su, "Crystal structure of p38 mitogen-activated protein kinase", *J. Biol. Chem.*, Vol. 271, pp. 27696–27700, 1996.
- [2] R. J. Davis, "Transcriptional regulation by MAP kinases", *Mol. Reprod. Dev.*, Vol. 42, pp. 459-467, 1995.
- [3] A. Kaieda, M. Takahashi, T. Takai, M. Goto, T. Miyazaki, Y. Hori, S. Unno, T. Kawamoto, T. Tanaka, S. Itono, T. Takagi, T. Hamada, M. Shirasaki, K. Okada, G. Snell, K. Bragstad, B. C. Sang, O. Uchikawa, and S. Miwatashi, "Structure-based design, synthesis, and biological evaluation of imidazo[1,2-b]pyridazine-based p38 MAP kinase inhibitors", *Bioorg. Med. Chem.*, Vol. 26, pp. 647-660, 2018.
- [4] Z. Wang, P. C. Harkins, R. J. Ulevitch, J. Han, M. H. Cobb, and E. J. Goldsmith, "The structure of mitogen-activated protein kinase p38 at 2.1-Å resolution", *Proc. Natl. Acad. Sci. U.S.A.*, Vol. 94, pp. 2327-2332, 1997.
- [5] X. Z. Wang and D. Ron, "Stress-induced phosphorylation and activation of the transcription factor CHOP (GADD153) by p38 MAP Kinase", *Science*, Vol. 272, pp. 1347-1349, 1996.
- [6] D. R. Knighton, J. H. Zheng, L. F. Ten Eyck, V. A. Ashford, N. H. Xuong, S. S. Taylor, and J. M. Sowadski, "Crystal structure of the catalytic subunit of cyclic adenosine monophosphate-dependent protein kinase", *Science*, Vol. 253, pp. 407-414, 1991.
- [7] J. M. Kyriakis and J. Avruch, "Mammalian mitogen-activated protein kinase signal transduction pathways activated by stress and inflammation", *Physiol. Rev.*, Vol. 81, pp. 807-869, 2001.
- [8] P. K. Balasubramanian, A. Balupuri, and S. J. Cho, "3D-QSAR studies on disubstituted dibenzosuberone derivatives as p38 α MAP kinase inhibitors using CoMFA and COMSIA", *Med. Chem. Res.*, Vol. 25, pp. 2349-2359, 2016.
- [9] B. Derijard, J. Raingeaud, T. Barrett, I. H. Wu, J. Han, R. J. Ulevitch, and R. J. Davis, "Independent human MAP-kinase signal transduction pathways defined by MEK and MKK isoforms", *Science*, Vol. 267, pp. 682-685, 1995.
- [10] J. Raingeaud, A. J. Whitmarsh, T. Barrett, B. Derijard, and R. J. Davis, "MKK3- and MKK6-regulated gene expression is mediated by the p38 mitogen-activated protein kinase signal transduction pathway", *Mol. Cell. Biol.*, Vol. 16, pp. 1247-1255, 1996.
- [11] A. Munshi and R. Ramesh, "Mitogen-activated protein kinases and their role in radiation response", *Genes Cancer*, Vol. 4, pp. 401-408, 2013.
- [12] R. J. Mayer and J. F. Callahan, "p38 MAP kinase inhibitors: A future therapy for inflammatory diseases", *Drug Discov. Today Ther. Strateg.*, Vol. 3, pp. 49-54, 2006.
- [13] J. C. Lee, S. Kumar, D. E. Griswold, D. C. Underwood, B. J. Votta, and J. L. Adams, "Inhibition of p38 MAP kinase as a therapeutic strategy", *Immunopharmacology*, Vol. 47, pp. 185-201, 2000.
- [14] M. Clark, R. D. Cramer III, and N. V. Opdenbosch, "Validation of the general purpose tripos 5.2 force field", *J. Comput. Chem.*, Vol. 10, pp. 982-1012, 1989.
- [15] R. Kumar, B. Långström, and T. Darreh-Shori, "Novel ligands of Choline Acetyltransferase designed by in silico molecular docking, hologram QSAR and lead optimization", *Sci. Rep.*, Vol. 6, p. 31247, 2016.